Journal of Current Science and Technology, May - August 2024 Vol. 14 No. 2, Article 36

ISSN 2630-0656 (Online)

Cite this article: Dechsri, K., Suwanchawalit, C., Apirakaramwong, A., Patrojanasophon, P., Rojanarata, T., Opanasopit, P., Pengnam, S., & Charoenying, T. (2024). Photo-sensitive antibacterial activity of *o*-phenylenediamine carbon dots. *Journal of Current Science and Technology*, *14*(2), Article 36. https://doi.org/10.59796/jcst.V14N2.2024.36

Journal of Current Science and Technology

Journal homepage: https://jcst.rsu.ac.th

Photo-sensitive Antibacterial Activity of *o*-Phenylenediamine Carbon Dots

Koranat Dechsri[1], Cheewita Suwanchawalit[2], Auayporn Apirakaramwong[3], Prasopchai Patrojanasophon[1], Theerasak Rojanarata[1], Praneet Opanasopit[1], Supusson Pengnam[1], and Thapakorn Charoenying[1*]

[1]Pharmaceutical Development of Green Innovations Group (PDGIG), Faculty of Pharmacy, Silpakorn University, Nakhon Pathom 73000, Thailand
[2]Department of Chemistry, Faculty of Science, Silpakorn University, Nakhon Pathom 73000, Thailand
[3]Department of Biomedicine and Health Informatics, Faculty of Pharmacy, Silpakorn University, Nakhon Pathom 73000, Thailand

*Corresponding author; E-mail: Charoenying_T@su.ac.th

Received 13 December,2023; Revised 21 January, 2024; Accepted 28 March, 2024
Published online 02 May, 2024

Abstract

Carbon dots (CDs) are among the famous nanoparticles that have been widely developed due to high biocompatibility, low toxicity, ease of preparation, excellent photoluminescent properties, and outstanding application in biomedicine. Among the various biomedical activities of CDs, they can be applied as antibacterial agents because of their photodynamic properties. Photodynamic therapy (PDT) has been considered an alternative antibacterial agent because of its non-invasive nature and minimal side effects, especially in terms of improving antibacterial activity against multidrug resistant bacteria when compared with traditional antibiotics. In this research, we developed CDs from *o*-phenylenediamine (OP). The *o*-phenylenediamine CDs (OPCDs) were synthesized via a hydrothermal method at 180°C for 3 h. After that, they revealed a spherical shape with a size range of 16.38 ± 2.64 nm. The minimum inhibitory concentration (MIC) and minimum bactericidal concentration (MBC) of OPCDs against *Staphylococcus aureus* (*S. aureus*) for both light exposure and without light exposure groups were significantly greater than the OP solution because the OPCDs could generate reactive oxygen species (ROS) via a photodynamic mechanism leading to the bacteria cell death. Therefore, the created OPCDs may have the capability to be utilized for treating skin infections caused mainly by *S. aureus.* In conclusion, OPCDs could be proposed as nanomaterials that enhance antibacterial activity and provide photodynamic properties.

Keywords**:** *antibacterial activity; carbon dots, o-phenylenediamine; photodynamic therapy; photosensitizers; reactive oxygen species; Staphylococcus aureus*

1. Introduction

The major cause of skin infectious diseases is *Staphylococcus aureus* (*S. aureus*), frequently found and recurrent in healthy and accessible personnel. Nowadays, there are considerable hurdles to the development of novel antibiotic drugs capable of effectively replacing traditional antibacterial therapies. The past ten years have seen a promising increase in the development of nanoparticles (NPs) used in a variety of biomedical applications, such as bioimaging, biosensing, drug delivery systems, and biomedical activity (Pandit et al., 2022). One of the biomedical activities used for treatments is the antibacterial activity (Pandit et al., 2022). The development of NPs, including magnetite NPs, zinc oxide NPs, silver NPs, gold NPs, carbon-based NPs (CNPs), and carbon dots (CDs) has been the subject of extensive research,

particularly in antibacterial applications (Diez-Pascual, 2018; Maťátková et al., 2022; Sweet, & Singleton, 2011).

Among various NPs, CDs have been considered as outstanding promised antibacterial properties because of their unique characteristics incorporating nano-scale range, low toxicity, great biocompatibility, inexpensive, water dispersibility, environmentally friendly, rapid synthesis, and easy functionalization (Hetta et al., 2023). In addition, CDs have been declared to be utilized as photodynamic therapy to improve antibacterial activity. It is also known as antibacterial photodynamic therapy (APDT). CDs perform as photosensitizers (PSs), which have enormous potential for fighting antibacterial resistance. They can absorb the visible spectrum and induce reactive oxygen species (ROS) such as hydroxyl radical (OH•), and singlet molecular oxygen ($^1O_2$) (Budimir et al., 2021). After that, ROS cause oxidative damage to intracellular biomolecules, influencing gene expression and ultimately leading to bacteria death. As a result, the phototherapy properties of CDs have been appealing for potential antibacterial applications (Sweet, & Singleton, 2011).

For this research, *o*-phenylenediamine (OP) was applied as a carbon precursor. The synthesis of CDs was prepared via the hydrothermal method because it has many advantages over other methods, such as convenience, easy operation, low cost, nontoxic, and high-yield production. After complete synthesis, CDs were collected to investigate the particle size and morphology via transmission electron microscopes (TEM). In addition, optical properties were investigated via ultraviolet-visible (UV-Vis) spectroscopy, and photoluminescence spectroscopy (PL). Subsequently, they were tested for antibacterial activity regarding minimum inhibitory concentration, minimum bacteriostatic concentration, bacterial viability, and photodynamic properties.

2. Objectives

In this work, we expected to fabricate CDs that can exhibit strong absorbance in the range of UV-Vis light, especially the Near-infrared (NIR) range. CDs that absorb suitable wavelengths can be applied for antibacterial activity against *S. aureus* via photodynamic therapy.

3. Materials and methods

3.1 Materials

The chemical reagents including OP, and 3-(4,5-Dimethyl-2-thiazolyl)-2,5-diphenyl-2H-tetrazolium bromide (MTT) were purchased from Sigma-Aldrich (St. Louis, MO, USA). Tryptic soy agar (TSA) and Tryptic soy broth (TSB) were obtained from Merck KGaA (Darmstadt, Germany) and Becton, Dickinson, and Company (MD, USA), respectively. *S. aureus* ATCC 6538P was utilized as a bacterial model for skin infection. Cell culture media, including Dulbecco's modified Eagle's medium (DMEM), penicillin-streptomycin, fetal bovine serum (FBS), and trypsin–EDTA were purchased from Gibco BRL (Rockville, MD, USA). The ultrapure water was prepared using a Milli-Q system (Millipore, USA). All other chemicals and solvents were used as received without purification.

3.2 Fabrication of carbon dots

The *o*-phenylenediamine CDs (OPCDs) were synthesized using OP as a carbon precursor via the hydrothermal method. In brief, OP was dissolved in deionized water with a controlled temperature of 80°C to attain the final concentration of 0.033 g/mL. After that, 30 mL of the prepared solution was transferred to a hydrothermal synthesis reactor model KH50 with a PTFE liner. Then the reactor was put in a hot air oven (FED720 Binder, BINDER GmbH, Tuttlingen, Germany) for synthesis with suitable conditions, including temperature at 180°C for 3 h. After the reaction was complete, the solution turned into a brown dispersion and was adjusted pH to 5.5-6.5, followed by centrifugation at 12000 rpm for 10 min and filtration with 0.22 μm membrane filter to eliminate the large NPs. Finally, the OPCD dispersion was lyophilized for 3 days and kept in a refrigerator at 4°C for future use.

3.3 Characterization of carbon dots

The morphology and particle size of the synthesized OPCDs were investigated via a transmission electron microscope (TEM; Philips TECNAI 20, Philips Ltd., USA) with a voltage of 100 kV and magnification of 175k. The preparation step was conducted before the OPCDs were observed by dropping them on a copper grid and drying them overnight at room temperature. The particle size was analyzed from different areas with normal distribution and presented as mean ± S.D. The UV-Vis spectra of OPCDs and OP solution were recorded through a UV-V is scanning

spectrophotometer by scanning within the wavelength range of 300 to 700 nm (Cary 60 UV-Vis, Agilent Technologies, USA). The excitation-dependent emission spectra of the OPCD dispersion were analyzed using a Spectro fluorophotometer by excitation within the wavelength range of 360 to 580 nm (RF-6000, Bara Scientific Co., Ltd., Shimadzu, Japan). For all spectrophotometry experiments, OPCDs were prepared at a concentration of 1 mg/mL.

3.4 Normal Human Fibroblast (NHF) Cell Viability

3.4.1 Cell cultures

Normal Human Fibroblast (NHF) cell lines were maintained in controlled incubators with 37°C and 5% carbon dioxide (CO_2) in culture medium, DMEM including 10% FBS and 1% penicillin-streptomycin. The cultured cells were observed through an inverted microscope (Nikon® T-DH, Nikon, Tokyo, Japan) to reach a 70–80% confluency for sub-culturing cells.

3.4.2 Cell viability

The cell viability of NHF incubated at various concentrations of OPCDs was determined through an MTT assay. Before being incubated, NHF cells were seeded at a density of 1×10^4 cells per well in 96-well culture plates. NHF cells were incubated at 37˚C, in a 5% CO_2 atmosphere for 24 h. The medium was then replaced with OPCDs at various concentrations (0.125, 0.25, 0.5, 1.0, and 2.0 mg/mL) and further incubated continuously for 24 h. Cell viability was assessed by adding 25 µL of MTT solution at 5 mg/mL of concentration in each well and further incubating for 3 h to develop formazan crystals in live cells. Subsequently, all the medium in each well was replaced with 100 µL of dimethyl sulfoxide (DMSO) to dissolve the crystals, and the solution changed to a bluish-violet color. Finally, the signal at the absorbance (Abs.) of 550 nm was investigated through a microplate reader. The cell viability was calculated using equation (1):

$$\text{Cell viability (\%)} = \frac{\text{Abs. of sample - Abs. of blank}}{\text{Abs. of control - Abs. of blank}} \times 100\% \quad (1)$$

3.5 Evaluation of antibacterial activity

3.5.1 Bacterial cultures

S. aureus was cultured in TSB medium in a bacterial incubator (Contherm digital series incubator, Contherm Scientific Ltd, Lower Hutt, New Zealand) at 37°C, 180 revolutions per minute (rpm) for 24 h. After that, the optical density of bacteria suspension was measured at 600 nm by using a microplate reader (VICTOR Nivo™ Multimode Plate Reader, PerkinElmer, Germany) to obtain the 0.5 McFarland standard. All pieces of equipment were sterilized by autoclaving at 121°C for 30 min to confirm sterility.

3.5.2 Minimum Inhibitory Concentration (MIC)

The MIC of OPCDs was evaluated through a broth dilution method. Briefly, A OPCDs dispersion was diluted in a 2-fold serial pattern to attain various concentrations (0.03125, 0.0625, 0.125, 0.25, 0.5, and 1.0 mg/mL) in a 24-well plate. Then, 10 µL of prepared bacterial suspensions were added into 990 µL of sample solutions to acquire the final concentration of bacteria at 10^6 colony-forming units per milliliter (CFU/mL). The samples were set up with 2 different conditions, (1) with and (2) without visible light exposure (0.12 W/cm^2), for 10 min to investigate the effect of visible light on the antibacterial activity. After that, the mixtures were incubated at 37˚C for 24 h to investigate the MIC values of the OPCDs. The lowest concentration of OPCDs without turbidity was observed and reported as MIC. Moreover, the MIC of the OP solution was also evaluated using a similar procedure.

3.5.3 Minimum Bactericidal Concentration (MBC)

The clear solutions of OP solution and OPCDs from the MIC study were chosen for MBC evaluation by spread plate method. Briefly, 100 µL of the samples were spread onto the agar plates. Then, all agar plates were incubated at 37˚C for 24 h. The lowest concentration of agar plates without any colonies was observed as MBC.

3.6 Evaluation of the bacterial viability

The antibacterial activity of OPCDs was investigated via a standard plate counting method adopted from a previously published protocol (Qie et al., 2022). In brief, 100 µL of 10^6 CFU/mL bacterial suspension and 400 µL of 200 µg/mL OPCD dispersion were mixed in a centrifuge tube and cultured at 37˚C for 3 h. Then the mixture dispersion was either exposed or non-exposed to visible light (0.12 W/cm^2) for 10 min. Phosphate-

buffered saline (PBS) was used as a negative control in the experiment. After that, the mixture solution was diluted 10-fold with PBS and 20 µL of the sample was spread onto agar plates. All plates were cultured at 37°C for 16 h. The number of bacterial was counted and calculated as bacterial viability according to equation (2):

$$\text{Bacterial viability (\%)} = \frac{N_e}{N_c} \times 100\% \qquad (2)$$

where N_e and N_c are the colony number of the sample and control (PBS with non-exposed), respectively.

3.7 Evaluation of the photodynamic capacity

To further investigate the formation of singlet oxygen ($^1O_2$), 1,3-diphenylisobenzofuran (DPBF) was applied as a trapping agent, which was modified from the previous study (Feng et al., 2020). Briefly, DPBF was dissolved in ethanol solution to obtain the final concentration at 1.35 mg/mL. The 50 µL of DPBF solution was mixed with 200 µL of OPCD dispersion (200 µg/mL). The mixture was then exposed to visible light at a power density of 0.12 W/cm^2 for 10 min. After that, 100 µL of the mixture solution was put into a 96-well plate to measure the absorbance of DPBF at 430 nm with a microplate reader. The distilled water was used as a negative control.

3.8 Statistical analysis.

Each experiment was performed in triplicate. The results were reported as mean ± S.D. All data was statistically analyzed by the independent *t*-test and *F*-test, which was conducted using IBM SPSS Statistics version 28 at a 95% confidence level (CI). Significant differences were defined at $p < 0.05$.

4. Results and discussion

4.1 Characterization of carbon dots

The schematic representation of the synthesis of OPCDs is presented in Figure 1. The particle size and morphology of the OPCDs were investigated via TEM. As shown in Figure 2a, the particle size of OPCDs was reported as 16.38 ± 2.64 nm, exhibiting a spherical shape, consistent with the previous reports (Liu et al., 2021; Mansuriya, & Altintas, 2021). As shown in Figure 2b, the UV-Vis spectrum of OPCDs (orange line) exhibited an absorbance peak at 425 nm, extended to 700 nm. The absorbance peak at 425 nm could be the π-π* and n-π* transition of the C = C and C = N bond (Mura et al., 2020). Meanwhile, the OP solution (blue line), used as a precursor, did not show any peaks. The difference in UV-Vis spectra between the OP solution and OPCDs could confirm the completion of the CD synthesis reaction. These results corresponded with the previous report (Ehtesabi, & Massah, 2021). Finally, the photoluminescence spectra of OPCDs were investigated, as shown in Figure 2c. The fluorescence emission intensity was recorded by excitation from 360 to 580 nm. The strongest fluorescence emission centered at 580 nm was observed when the excitation wavelength was 420 nm. The results showed that OPCDs exhibited a red shift of fluorescence emission when compared to the previous reports of CDs, which showed a blue fluorescence. This difference in carbon sources may affect core structural differences or functional groups present on the surface of CDs that could contribute to phenomenon shift. Previous reports usually use citric acid as a carbon source. In contrast, this study selected the *o*-phenylenediamine, which serves as a carbon and nitrogen source, contributing to the presence of nitrogen groups on the surface and resulting in a red shift in fluorescence emission (Duan et al., 2019; Kong et al., 2018; Liu et al., 2012; Wang et al., 2020; Yu et al., 2022).

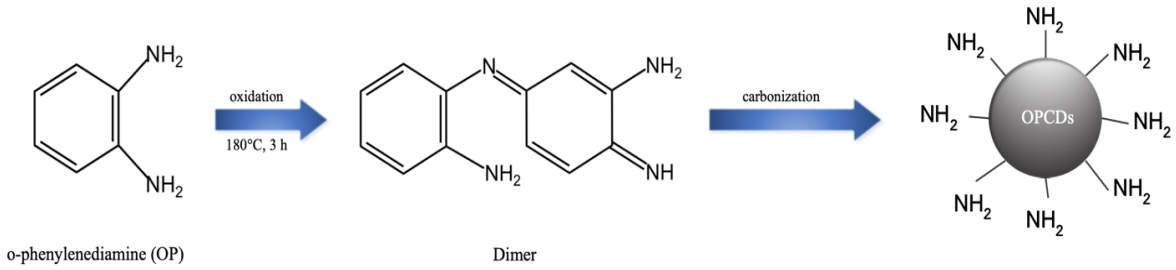

Figure 1 Schematic representation of the synthesis of OPCDs from *o*-phenylenediamine (OP)

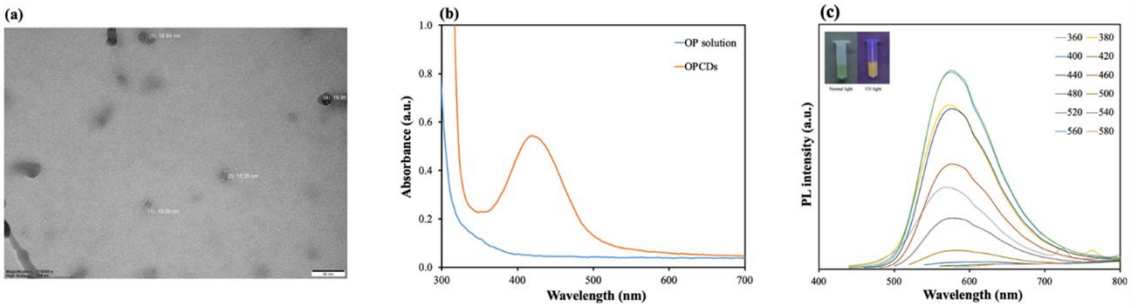

Figure 2 Characterization of OPCDs: (a) TEM image; (b) UV-vis spectra; (c) photoluminescence (PL) spectra (inset: photographs of OPCDs solution under normal and UV light)

Table 1 MIC and MBC of OPCDs and OP solution with or without visible light exposure (0.12 W/cm^2) for 10 min against *S. aureus*

Samples	Without light exposure		Light exposure	
	MIC (mg/mL)	MBC (mg/mL)	MIC (mg/mL)	MBC (mg/mL)
OP solution	2.08	8.33	1.04	2.08
OPCDs	0.125	0.125	0.0625	0.0625

4.2 Cell viability

The cell viability of NHF cells after being treated with OPCDs for 24 h was estimated using an MTT assay, as shown in Figure 3. The untreated cells reported as the control represented 100% cell viability. For cell viability of the treatment groups, all the concentrations in the range of 0.125-2.0 mg/mL could retain cell viability more than 80%. Therefore, it can be reported that the OPCDs were biocompatible with fibroblast cells.

4.3 Antibacterial activity of the CDs

The antibacterial activity of OPCDs was examined via a broth microdilution method and the spread plate technique to obtain the MIC and MBC against *S. aureus*. As shown in Table 1, the MIC and MBC values of the OPCDs for both light exposure and without light exposure groups were significantly lower than those of the OP solution. In addition, due to the effect of light exposed OPCDs, the OPCDs could absorb the visible wavelength implying the result of UV absorption in Figure 2b, and then they induce ROS which can affect bacteria death. Hence, OPCDs that were exposed to light exhibited lower MIC, and MBC significantly than OP solution. This may be due to the particle size in the nano range of OPCDs; they might activate the distribution into the cell membrane of bacteria via lipid bilayer and exhibit greater antibacterial activity than the OP solution. Furthermore, the outer membrane or cell wall of bacteria was disrupted by OPCDs, leading to bacterial cellular dysfunction and the cytoplasm leak, causing bacteria cell death (Mosquera et al., 2018; Xin et al., 2019). In addition, the MIC, and MBC that were effective for the antibacterial application of OPCDs without and with light exposure were reported at about 0.125 and 0.0625 mg/mL, respectively. According to the NHF viability assessment, the result reported the maximum OPCDs concentration caused the NHF viability that was not significantly different from the control sample was 0.25 mg/mL. Hence, the maximum effective concentration without harming the NHF was higher than the MIC and the MBC against *S. aureus*. Therefore, OPCDs exhibited a potential candidate that can apply for an antibacterial application.

Bacterial viability was determined using a standard plate counting method to further evaluate the effect of light exposure on the antibacterial activity of OPCDs. The bacterial viability of the control group (PBS) remained greater than 80% for both conditions (with and without light exposure), as shown in Figure 4. The bacterial viability of the OPCDs without being exposed to visible light was 74.94 ± 7.07%. In contrast, the bacterial viability of the OPDCs exposed to light dramatically declined to 15.26 ± 6.24% because ROS were activated via the photodynamic properties (Qie et al., 2022) since the OPCDs could absorb visible light (Figure 2b) and act as PSs (Diez-Pascual, 2018; Hu et al., 2018).

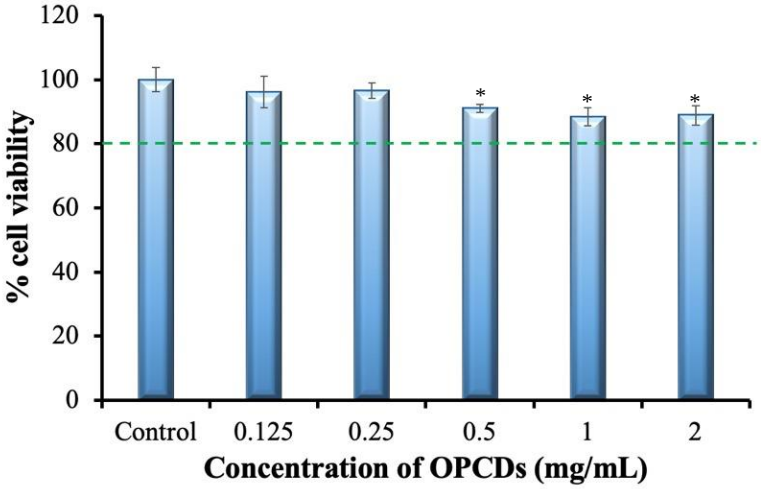

Figure 3 Cell viability of NHF cells after treated with OPCDs at different concentrations for 24 h. *Significant difference from the control at $p < 0.05$

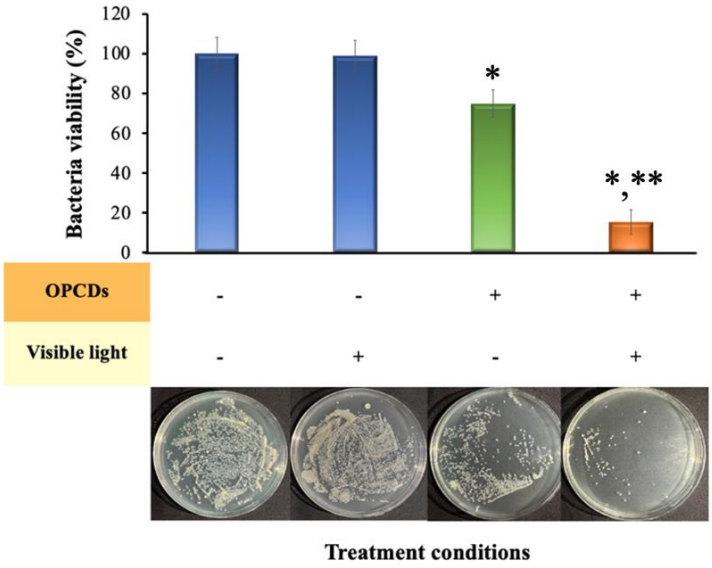

Figure 4 The bacterial viability of *S. aureus* by a standard plate counting method with different treatment conditions (- absence, + presence). *Significant difference from the control, **Significant difference from the nonexposed light of OPCDs at $p < 0.05$

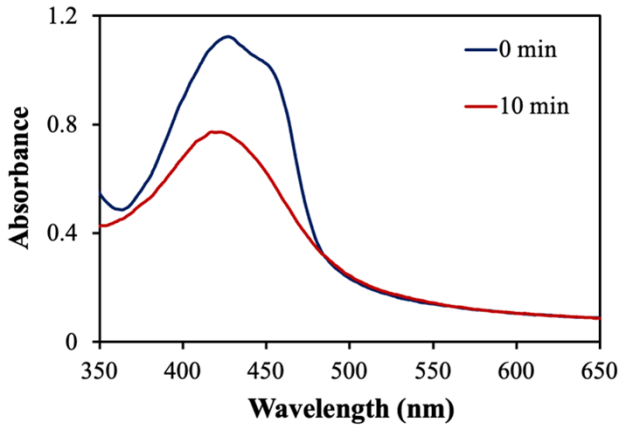

Figure 5 The UV-vis spectra of DBPF mixed with OPCDs at different light exposure times, 0 and 10 min

4.4 Detection of ROS

ROS generation was assessed by observing the decrease in absorbance intensity of a trapping agent (DPBF), as depicted in Figure 5. The absorbance intensity of DPBF significantly decreased after light exposure for 10 min, which corresponded to the previous report (Bhattacharyya et al., 2018). Because DPBF reacts with singlet oxygen induced by OPCDs, it undergoes a photochemical reaction known as a Diels-Alder reaction, a (4 + 2) cycloaddition reaction. This reaction involves the addition of singlet oxygen to one of the double bonds in the DPBF molecule, followed by a rearrangement to form an endoperoxide intermediate. This intermediate then undergoes further rearrangement to yield a stable product, which is no longer capable of absorbing light at the same wavelength (Li et al., 2017). The result confirmed that the OPCDs could generate ROS and might damage proteins, fatty acids, and other macromolecules, which can cause bacterial cell death.

5. Conclusion

In summary, OPCDs were successfully synthesized using a one-pot hydrothermal technique. The as-prepared OPCDs exhibited biocompatibility with NHF cells, showed strong antibacterial activity against *S. aureus* compared to the OP solution, and presented excellent photodynamic properties, which could be applied as PSs to enhance antibacterial activity via generating ROS. Consequently, the OPCDs offered promising nanomedicine to enhance antibacterial activity, with potential applications in treating skin infections primarily caused by *S. aureus*.

6. Acknowledgements

This research project is supported by National Research Council of Thailand (NRCT): (Contact No. N41A661126 and N42A650551). Besides that, we would like to thank undergraduate students: Pimlapat Naulsanong, Proeksa Autsawahloowarapong, and Thitiporn Sripanya for possessing assistance.

7. References

Bhattacharyya, A., Jameei, A., Garai, A., Saha, R., Karande, A. A., & Chakravarty, A. R. (2018). Mitochondria-localizing BODIPY-copper(ii) conjugates for cellular imaging and photo-activated cytotoxicity forming singlet oxygen. *Dalton Transactions*, *47*(14), 5019-5030. https://doi.org/10.1039/C8DT00255J

Budimir, M., Marković, Z., Vajdak, J., Jovanović, S., Kubat, P., Humpoliček, P., ... & Marković, B. T. (2021). Enhanced visible light-triggered antibacterial activity of carbon quantum dots/polyurethane nanocomposites by gamma rays induced pre-treatment. *Radiation Physics and Chemistry*, *185*, Article 109499. https://doi.org/10.1016/j.radphyschem.2021.109499

Diez-Pascual, A. M. (2018). Antibacterial Activity of Nanomaterials. *Nanomaterials (Basel)*, *8*(6), 359-364. https://doi.org/10.3390/nano8060359

Duan, Q., Ma, Y., Che, M., Zhang, B., Zhang, Y., Li, Y., ... & Sang, S. (2019). Fluorescent carbon dots as carriers for intracellular doxorubicin delivery and track. *Journal of Drug Delivery Science and Technology*, *49*, 527-533. https://doi.org/10.1016/j.jddst.2018.12.015

Ehtesabi, H., & Massah, F. (2021). Improvement of hydrophilicity and cell attachment of polycaprolactone scaffolds using green synthesized carbon dots. *Materials Today Sustainability*, *13*, Article 100075. https://doi.org/10.1016/j.mtsust.2021.100075

Feng, J., Chen, S., Yu, Y.-L., & Wang, J.-H. (2020). Red-emission hydrophobic porphyrin structure carbon dots linked with transferrin for cell imaging. *Talanta*, *217*, Article 121014. https://doi.org/10.1016/j.talanta.2020.121014

Hetta, H. F., Ramadan, Y. N., Al-Harbi, A. I., A. Ahmed, E., Battah, B., Abd Ellah, N. H., ... & Donadu, M. G. (2023). Nanotechnology as a Promising Approach to Combat Multidrug Resistant Bacteria: A Comprehensive Review and Future Perspectives. *Biomedicines*, *11*(2), 413-435. https://doi.org/10.3390/biomedicines11020413

Hu, X., Huang, Y. Y., Wang, Y., Wang, X., & Hamblin, M. R. (2018). Antimicrobial Photodynamic Therapy to Control Clinically Relevant Biofilm Infections. *Frontiers in Microbiology*, *9*, Article 1299. https://doi.org/10.3389/fmicb.2018.01299

Kong, T., Hao, L., Wei, Y., Cai, X., & Zhu, B. (2018). Doxorubicin conjugated carbon dots as a drug delivery system for human breast cancer therapy. *Cell Proliferation*, *51*(5), Article e12488. https://doi.org/10.1111/cpr.12488

Li, Z., Liu, C., Abroshan, H., Kauffman, D. R., & Li, G. (2017). Au38S2(SAdm)20 Photocatalyst for One-Step Selective Aerobic Oxidations. *ACS Catalysis*, *7*(5), 3368-3374. https://doi.org/10.1021/acscatal.7b00239

Liu, C., Zhang, P., Zhai, X., Tian, F., Li, W., Yang, J., ... & Liu, W. (2012). Nano-carrier for gene delivery and bioimaging based on carbon dots with PEI-passivation enhanced fluorescence. *Biomaterials*, *33*(13), 3604-3613. https://doi.org/10.1016/j.biomaterials.2012.01.052

Liu, Y., Roy, S., Sarkar, S., Xu, J., Zhao, Y., & Zhang, J. (2021). A review of carbon dots and their composite materials for electrochemical energy technologies. *Carbon Energy*, *3*(5), 795-826. https://doi.org/10.1002/cey2.134

Mansuriya, B. D., & Altintas, Z. (2021). Carbon Dots: Classification, Properties, Synthesis, Characterization, and Applications in Health Care-An Updated Review (2018-2021). *Nanomaterials (Basel)*, *11*(10), 2525-2579. https://doi.org/10.3390/nano11102525

Maťátková, O., Michailidu, J., Miškovská, A., Kolouchová, I., Masák, J., & Čejková, A. (2022). Antimicrobial properties and applications of metal nanoparticles biosynthesized by green methods. *Biotechnology Advances*, *58*, Article 107905. https://doi.org/10.1016/j.biotechadv.2022.107905

Mosquera, J., Garcia, I., & Liz-Marzan, L. M. (2018). Cellular Uptake of Nanoparticles versus Small Molecules: A Matter of Size. *Accounts of Chemical Research*, *51*(9), 2305-2313. https://doi.org/10.1021/acs.accounts.8b00292

Mura, S., Ludmerczki, R., Stagi, L., Garroni, S., Carbonaro, C. M., Ricci, P. C., ... & Innocenzi, P. (2020). Integrating sol-gel and carbon dots chemistry for the fabrication of fluorescent hybrid organic-inorganic films. *Scientific Reports*, *10*(1), 4770-4781. https://doi.org/10.1038/s41598-020-61517-x

Pandit, C., Roy, A., Ghotekar, S., Khusro, A., Islam, M. N., Emran, T. B., ... & Bradley, D. A. (2022). Biological agents for synthesis of nanoparticles and their applications. *Journal of King Saud University - Science*, *34*(3), Article 101869. https://doi.org/10.1016/j.jksus.2022.101869

Qie, X., Zan, M., Gui, P., Chen, H., Wang, J., Lin, K., ... & Song, Y. (2022). Design, Synthesis, and Application of Carbon Dots With Synergistic Antibacterial Activity. *Front Bioeng Biotechnol*, *10*, Article 894100. https://doi.org/10.3389/fbioe.2022.894100

Sweet, M., & Singleton, I. (2011). Silver nanoparticles: a microbial perspective. *Advances in Applied Microbiology*, *77*, 115-133. https://doi.org/10.1016/B978-0-12-387044-5.00005-4

Wang, S., Chen, L., Wang, J., Du, J., Li, Q., Gao, Y., ... & Yang, Y. (2020). Enhanced-fluorescent imaging and targeted therapy of liver cancer using highly luminescent carbon dots-conjugated foliate. *Materials Science and Engineering: C*, *116*, Article 111233. https://doi.org/10.1016/j.msec.2020.111233

Xin, Q., Shah, H., Nawaz, A., Xie, W., Akram, M. Z., Batool, A., ... & Gong, J. R. (2019). Antibacterial Carbon-Based Nanomaterials. *Advanced Materials*, *31*(45), Article e1804838. https://doi.org/10.1002/adma.201804838

Yu, R., Liang, S., Ru, Y., Li, L., Wang, Z., Chen, J., & Chen, L. (2022). A Facile Preparation of Multicolor Carbon Dots. *Nanoscale Research Letters*, *17*(1), Article 32. https://doi.org/10.1186/s11671-022-03661-z